Int J Earth Sci (Geol Rundsch) (2017) 106:2429–2444
DOI 10.1007/s00531-016-1439-4

ORIGINAL PAPER

Fluid geochemistry of the Mondragone hydrothermal systems (southern Italy): water and gas compositions vs. geostructural setting

Emilio Cuoco[1] · Angelo Minissale[2] · Antonella "Magda" Di Leo[3] · Stella Tamburrino[3] · Marina Iorio[3] · Dario Tedesco[1]

Received: 5 August 2015 / Accepted: 20 December 2016 / Published online: 23 February 2017

Abstract The geochemistry of natural thermal fluids discharging in the Mondragone Plain has been investigated. Thermal spring emergences are located along the Tyrrhenian coast in two different areas: near Padule-S. Rocco (41°7.5′N 13°53.4′E) at the foot of Mt. Petrino, and near Levagnole (41°8.5′N 13°51.3′E) at the foot of Mt. Pizzuto. The water isotopic composition of both thermal discharges is lighter than the one of local shallow groundwater ($\delta^{18}O \cong -6.3‰$ SMOW vs. $\cong -5.9‰$; $\delta D \cong -40‰$ SMOW vs. $\cong -36‰$, respectively) as a consequence of inland higher altitude of recharge by rainfall, suggesting that thermal water undergoes a deep and long flow-path before emerging along the coast. The chemical composition of the highest temperature samples of two areas points that fluids in the hydrothermal reservoir(s) interact with similar lithologies, since they are both hosted in the lower sedimentary carbonate formations of the Campanian–Latial Apennine succession. However, the two spring systems are different in terms of temperature and salinity (Levagnole: ≅50 °C and 8.9 g/L vs. Padule: ≅32 °C and 7.4 g/L, respectively). The higher salinity of Levagnole springs is due to a longer interaction with evaporite material embedded in Miocene sedimentary formations and to the eventual mixing, during rising, with fresh seawater close to the seashore. The chemical and isotopic composition of the free gases associated with the springs, again suggests a different source of the two hydrothermal systems. Comparing the $^3He/^4He$ measured ratios with other gas emissions located NE and SE of Mt. Massico-Roccamonfina alignment, it is evident that the Levagnole thermal springs are related to the northern Latial mantle wedge where the $^3He/^4He$ is about 0.5 *R*/Ra, whereas the Padule-S. Rocco springs, although being only 3.5 km south of Levagnole, are related to the Campanian mantle wedge where *R*/Ra is always ≥2.0. Such a difference in $^3He/^4He$ ratio in a very short distance, clearly, suggests a different source of the Padule-S.Rocco gas phase rising to the surface through the deep transpressive regional fault(s) system related to the NE–SW Ortona–Roccamonfina tectonic alignment.

Keywords Mondragone Plain · Thermal waters · Water and gas geochemistry · Peri-Tyrrhenian belt geodynamics · VIGOR project

Electronic supplementary material The online version of this article (doi:10.1007/s00531-016-1439-4) contains supplementary material, which is available to authorized users.

✉ Emilio Cuoco
cuoco@unina2.it

[1] Department of Environmental, Biological and Pharmaceutical Sciences and Technologies, Second University of Naples, Via A. Vivaldi 43, 81100 Caserta, Italy

[2] C.N.R. (Italian Council for Research), Institute of Geosciences and Earth Resources, Via G. La Pira 4, 50121 Florence, Italy

[3] C.N.R. (Italian Council for Research), Institute for Coastal Marine Environment, Calata Porta di Massa, 80133 Naples, Italy

Introduction

The Peri-Tyrrhenian belt of central/southern Italy and the Tyrrhenian Sea is affected by intense volcanism and related geothermal anomalies (Cataldi et al. 1995; Minissale 2004; Chiodini et al. 2013). The Pliocene–Quaternary extensional tectonic regime and the anticlockwise rotation of the Apennines triggered crustal fracturing and magma rising through anti-Apennine normal faults (Ferranti et al. 1995), which were re-activated from older transcurrent ones (Italiano

et al. 2000). Important volcanic districts, which migrated from the northern Apennines (Tuscany) in the Pliocene to the southern Neapolitan area (still active), have intensely been investigated in the past two decades (Peccerillo 2001; Conticelli et al. 2002; Ciotoli et al. 2003; Cimarelli and; De and Rita 2006; Panza et al. 2007; Rouchon et al. 2008). Natural hydrothermal manifestations in Tuscany and Latium have also been largely investigated, even in recent time (Di Filippo et al. 1999; Gambardella et al. 2004; Frondini et al. 2008, 2009; Tassi et al. 2012; Chiodini et al. 2013; Gasparrini et al. 2013; Corrado et al. 2014). In particular, the origin of CO_2 and the relation between CO_2 emissions, thermal springs, and travertine deposits have been reviewed by Minissale (2004 and references therein). In spite of such intense research activity, hydrothermal fluids emissions in the northern sector of the Campania region (30 km NNW of Naples, Fig. 1) have not been sufficiently investigated. The main structure of this area is the Roccamonfina Volcano (1005 m in elevation, active from about 550 to 150 kyr BP; Rouchon et al. 2008), where several thermal springs and CO_2-rich waters are present (Fig. 1).

Among the limited number of research papers on these hydrothermal manifestations, Giordano et al. (1995) investigated the Riardo mineral waters (a bottled sparkling water known as "*Ferrarelle*"); D'Amore et al. (1995) studied the Suio hydrothermal system located at the northern slope of the Roccamonfina Volcano (Figs. 1, 2), and Duchi et al. (1995) and Corniello (1988) discussed the chemical composition (major ions) of several mineral springs in the Roccamonfina surroundings (i.e.: Pratella, Riardo, Francolise, Mondragone, and Suio; Figs. 1, 2), which have been related to the residual hydrothermal activity of the Roccamonfina

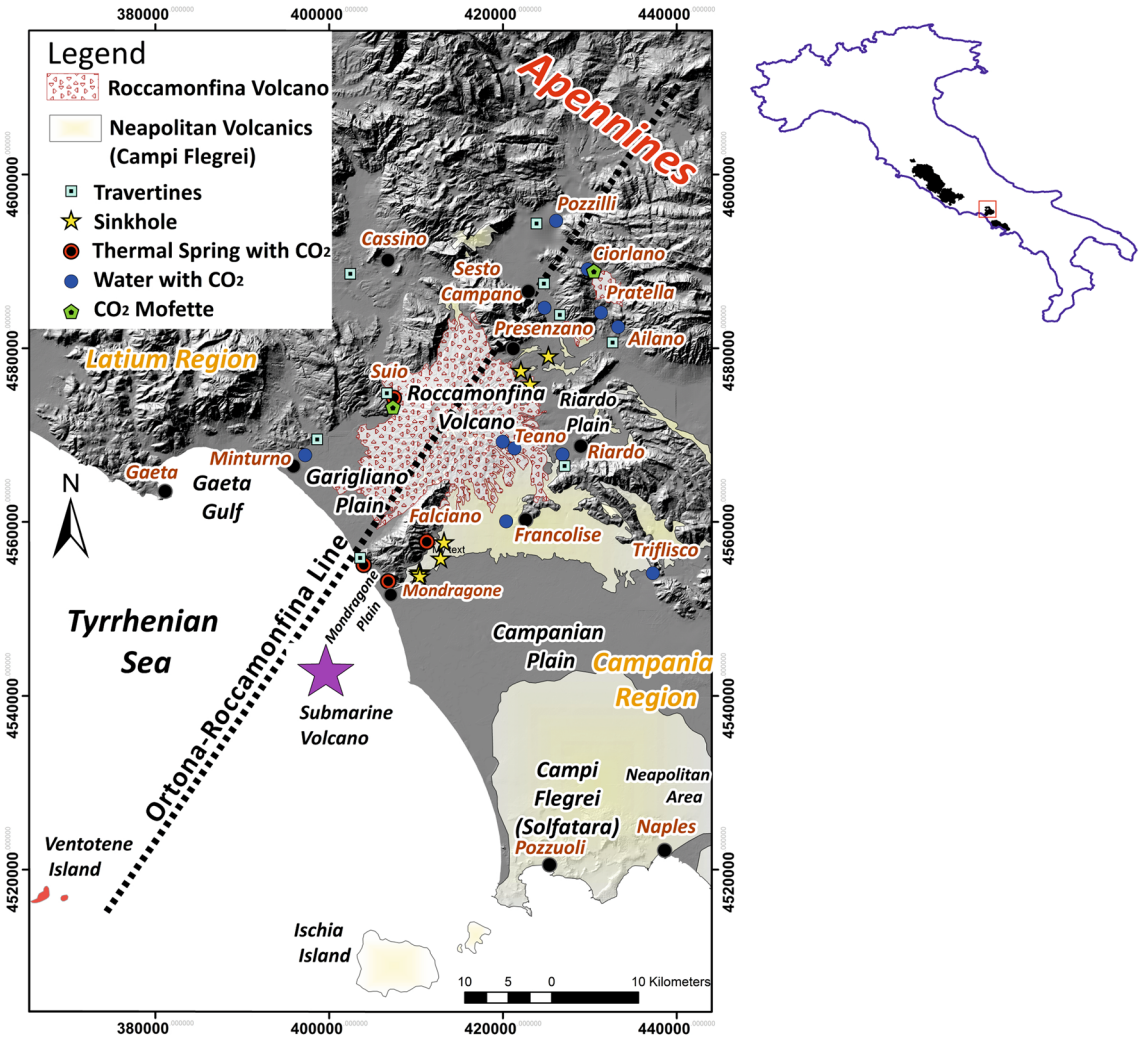

Fig. 1 Geographical framework of the investigated area; the *black shaped areas* are peri-tyrrhenian volcanic areas in the Italian peninsula. The regional distribution of CO_2-saturated springs, gas emissions, volcanic edifices, travertine deposits, and sinkholes are also reported. Plotted thermal and volcanic features match the Ortona–Roccamonfina alignment (ORL)

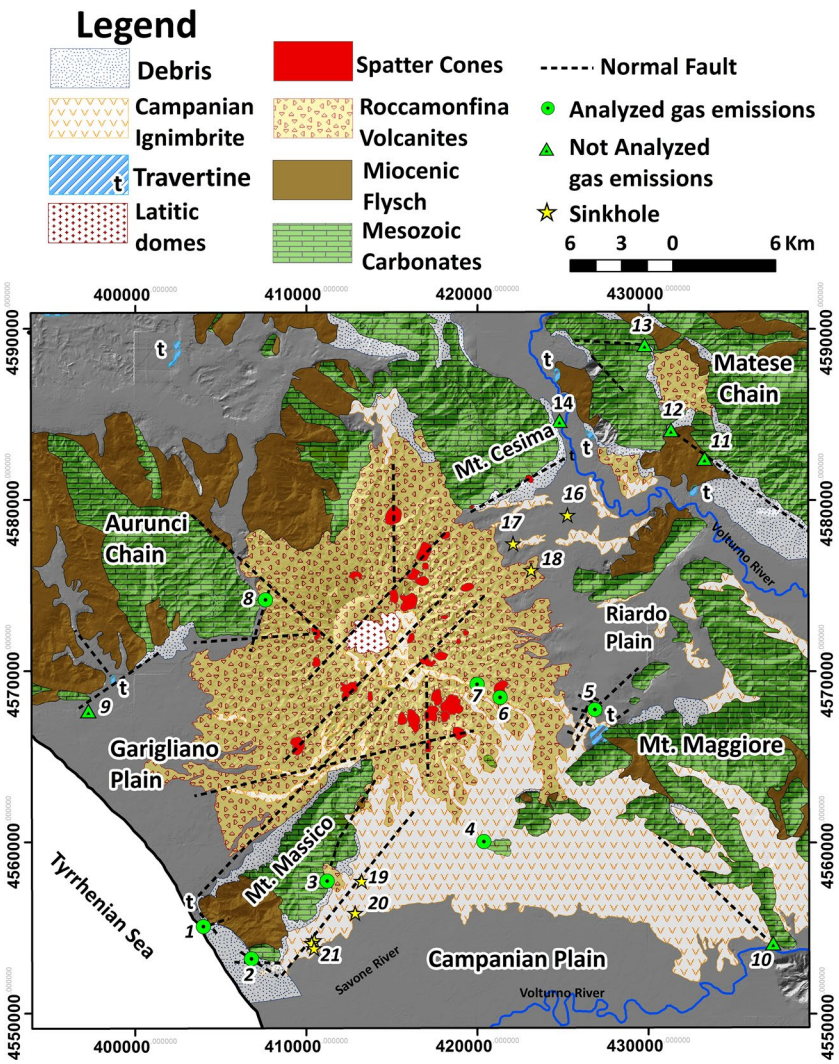

Fig. 2 Geological setting of the investigated area. Recent alluvial formations have not been reported. Normal faults (whose positions are derived from references cited in the text) match the location of lateral eruption from the Roccamonfina Volcano, of the hydrothermal springs in its surroundings and of the sinkholes. Gas emissions are mostly from CO_2-saturated water from springs and wells: *1* Levagnole (Mondragone), *2* Padule-S. Rocco (Mondragone), *3* Falciano del Massico, *4* Acqua Calena (Francolise), *5* Riardo Mineral Waters, *6* Acqua Ferrata (Teano), *7* Furnolo (Teano), *8* Suio, *9* Minturno, *10* Triflisco, *11* Ailano, *12* Pratella, *13* Ciorlano, *14* Sesto Campano. Sinkholes: *16* Lago di Vairano, *17* Aia Spaccata, *18* Lago delle Coree, *19* Fossa dell'Annunziata, *20* Lago di Falciano, *21* Fossa del Ballerino–Fossa Barbata–Fossa della Torre

Volcano. Recent studies focusing on the Mondragone thermal springs (Corniello et al. 2015; Cuoco et al. 2015) have demonstrated that thermal waters spread into shallow unconfined aquifer(s) after rising from a deep confined carbonate sedimentary aquifer.

The geographical and geological overview of the area (Figs. 1, 2) allows to identify, apart from the Roccamonfina volcano: (1) a small eruptive centre intruded the Mt. Cesima carbonate relief in proximity of Presenzano (Di Girolamo et al. 1991); (2) a clear alignment of CO_2-rich springs in the NE-SW direction matching the Mt. Massico normal faults direction; (3) the occurrence of sink holes and travertine deposits along the same direction (Del Prete et al. 2004); and (4) volcano-tectonic episodes related with a submarine volcano located in the Gaeta Gulf (De Rita et al. 1986; Bruno et al. 2000; De Alteriis et al. 2006). The distribution of these features matches the direction of the SW–NE Ortona–Roccamonfina Line (ORL), a transpressive regional fault cutting the entire Apennines (Milano et al. 2008), where geodynamic movements have likely driven magmatic mantle magmas into the shallow crust (De Rita and Giordano 1996). The role of active faults (including ORL) in the Campanian volcanism has been also stressed by the previous studies (Rolandi et al. 2003; Piochi et al. 2005; Torrente et al. 2010).

The hydrothermal manifestations are placed in such a geodynamic context at the foot of the coastal branch of the Mt. Massico complex (Fig. 2), around the town of Mondragone. The spring named Levagnole (also known as *Casino di Tranzo* and *Sinuessa*) is located at the foot of Mt. Pizzuto, while the one named Padule-S. Rocco (known as *acqua sulfurea*) is located at the foot of Mt. Petrino. Levagnole (LEV) has been described by Duchi et al. (1995) and Corniello (1988), whereas the Padule-S. Rocco (PSR) has been only recently described by Corniello et al. (2015) and Cuoco et al. (2015).

The present investigation has been partially performed in the frame of the geothermal VIGOR project funded by

Italian Ministry of Economic Development, with the synergy of the Second University of Naples and the Institute of Coastal Areas (IAMC) of the Italian Council for Research (CNR). The study on the chemical and isotopic composition of water samples, partly discussed in Corniello et al. (2015), adds original data concerning the composition of major and minor elements and chemical composition of free gases emitted from wells, and isotopic composition for carbon ($\delta^{13}C\text{-}CO_2$) and helium ($^3He/^4He$ ratios expressed as *R*/Ra). The aim of this investigation is to improve the knowledge on the mineralization processes occurring within the aquifer(s) where the thermal springs emerge to the surface and to identify the sources of the emitted free gases to better describe the hydrothermal dynamics of the Mondragone area. For better understanding, sampling of gas emissions was extended to other areas in the Roccamonfina volcano surroundings (Fig. 1).

Geological setting

The Campania–Latium margin of the Tyrrhenian Sea belongs to the central-southern Apennine fold-and-thrust belt formed during the Miocene and still active (Mostardini and Merlini 1986). In the Mondragone area, the early Pliocene extensional tectonics locally displaced the chain, triggering the down throw of the Mesozoic–Cenozoic substratum toward the sea, which is prolonged westward in the structural depressions of the Gaeta Bay (Zitellini et al. 1984) and southward in the Campanian Plain (Milia et al. 2013). In this framework, an important regional tectonic structure in this sector of the chain, is the southern tip of the ORL, consisting in a dextral strike-slip fault system representing the surface expression of a deep lithosphere rifting (Cinque et al. 1993). This important tectonic alignment bounds the Mt. Massico, which is a horst separating the northern Garigliano Plain from the southern Campanian Plain (Fig. 2).

The stratigraphy of the structural heights recalls the pre-orogenic succession, i.e.: (1) Triassic–Jurassic carbonates (dolostone), (2) Cretaceous limestones and (3) lower-to-middle Miocene carbonate ramp deposits. Late Miocene formations, also present in the area, have been investigated by Cosentino et al. (2006) and Cipollari et al. (1999) through a 2000 m-deep explorative well in the Garigliano Plain. Results report, from the top: (1) marly claystones and siltstones with intercalations of sandstones, (2) clayey-marls with thin siltstones and sandstones intercalations, and followed by (3) grey clayey-marls in the last 200 m of drilling and layers of evaporite minerals. The Miocene formations cover the older Mesozoic carbonate successions and are the stratigraphic basement of the Roccamonfina Volcanic complex (Capuano et al. 1992). Being impermeable, the Miocene formations significantly constrain the groundwater circulation in the deep buried sectors of the carbonate Mesozoic aquifers.

The volcanic activity in the Campania region started at the intersection between NW–SE and NE–SW Pliocene–Quaternary grabens (De Rita and Giordano 1996; Acocella and Funiciello 2006). In particular, the activity of Roccamonfina (550–150 kyr BP) and Campi Flegrei (39 kyr BP) in the Neapolitan area proceeded in conjunction with the establishment of a high rate subsidence of the coastal terrains. During subsidence, shallow marine and lacustrine deposits filled the formed depressions, both at the Volturno Plain (Fig. 2; Ortolani and Aprile 1985; Romano et al. 1994), and at the Garigliano Plain (Fig. 2; Nicotera and Civita 1969). The resulting Neogene successions are very different in the two plains: the Volturno Plain thickness reaches 4000 m and buried lava domes have also been identified (Aiello et al. 2011), whereas at Garigliano, an explorative well drilled by the Italian Oil Company (AGIP) intercepted the sedimentary terrigenous basement at a shallow depth of 200 m (Cosentino et al. 2006).

The so-called "*Campanian Ignimbrite*", a widespread deposit emplaced by a Campi Flegrei eruption occurring 39 kyr BP, has covered the pyroclastic–alluvial deposits of the Campanian/Volturno Plain (Corniello et al. 2010), whereas in the northern Garigliano Plain, the most part of volcanic products belongs to the Roccamonfina Volcano (Ducci et al. 2010). The Mondragone Plain connects the two grabens and its stratigraphy reflects mostly that of the Volturno Plain (Corniello et al. 2010), even if the carbonate basement is here less subsided being at the edge of the Mt. Massico horst (Amoresano et al. 2015).

At the foot of Mt. Petrino, thermal water springs out from a hollow locally named *Padule*. The hollow consists of a topographic depression where the top of the carbonate basement reaches the shallowest depth at −30 m from the surface. The depression is filled by Holocene sediments and peat deposits, suggesting the presence of a lacustrine Paleo-environment (Amoresano et al. 2015; Corniello et al. 2015).

The thermal emergence near Levagnole at the foot of Mt. Pizzuto (LEV) springs out by the side of the Garigliano Plain, where the carbonate basement hosting the thermal aquifer is located at a depth of −27 m from the surface and is isolated from the shallow unconfined aquifer by clay-rich sediments. In this area, the Quaternary alluvial sediments and the pyroclastics of the Campanian ignimbrite host the shallow groundwater of the plain (Amoresano et al. 2015; Corniello et al. 2015).

Materials and methods

Description of the sampling sites

The location of the springs and that of the sampled wells are shown in Fig. 3 and have been divided in three groups.

The first group includes samples from #1 to #9 and was collected at Mt Pizzuto foot, i.e., in the *Levagnole* area (LEV). Samples #1, #2, #4, #5, and #6 are natural springs, while samples #3, #7, #8 and #9 are taken from wells, approximately 20–25 m deep. All sampling points are characterized by gas emission (bubbling gas) apart from wells #8 and #9, probably because the letter are located at higher elevation (~100 m a.s.l.) than the others (10–50 m a.s.l.), placed before the normal fault bordering Mt. Pizzuto.

The second group, characterized by water and gas (CO_2) emissions, is located in the Padule-S. Rocco (PSR) area at the foot of Mt. Petrino (Fig. 3); its sampling points are numbered from #11 to #17. The well #11, a 80 m-deep well under pressure, is the more representative site of the deep thermo-mineral reservoir of the PSR hydrothermal system, while the sampling points from #12 to #17 are shallower wells, originally drilled for irrigation. Most of these wells were abandoned due to the high saline content of the water, high gas concentrations, and high temperature. Well #16 is only 3 m deep and its water represents the shallow unconfined aquifer in the Mondragone Plain, even if it is anyhow affected by CO_2 gas bubbling.

The remaining sampling points group shallow wells having cold waters without gas emissions (CSG) belonging to the unconfined aquifer of the Mondragone plain. Samples from #18 to #24 are well drilled for irrigation purposes between LEV and PSR (*Incaldana* area); samples from #25 to #29 are located inside Mondragone town mostly used for domestic water supply; samples from #30 to #33 are again irrigation wells located in the countryside, south of the Mondragone urban area.

Sampling, field measurements, and laboratory analyses

Water temperature, *p*H, electric conductivity (EC_{20}, referring to a standard temperature of 20 °C), and redox potential (Eh) were measured in the field using portable instruments. Alkalinity was also measured in the field by in-situ titration with an HCl 0.1 N solution, using methyl orange as an indicator. Samples were filtered during field collection using 0.45 µm Millipore MF filters, stored in PE bottles and the ones intended for cations determination were acidified with Merck® ultra-pure HNO_3.

Major elements were analysed by ion chromatography, using a Dionex DX-120 on unfiltered water sample for F, Cl, Br, NO_3, and SO_4 determination, and filtered and acidified samples for Na, K, Mg, and Ca. All selected analyses yielded analytical errors <5%, based on charge balance. Data quality, in terms of accuracy, errors, and relative uncertainly, was already discussed in Pascale-Tommasone et al. (2011). Samples for ICP-MS have been prepared as reported in Cuoco et al. (2010, 2013a, b, c) and analysed using an Agilent 7500ce ICP-MS, with ORS technology (utilizing collision cell technology). The following elements were analysed: Li, B, Ba, Fe, Mn, Sr and Rb. The analytical and accuracy error was better than 10%. $^{18}O/^{16}O$

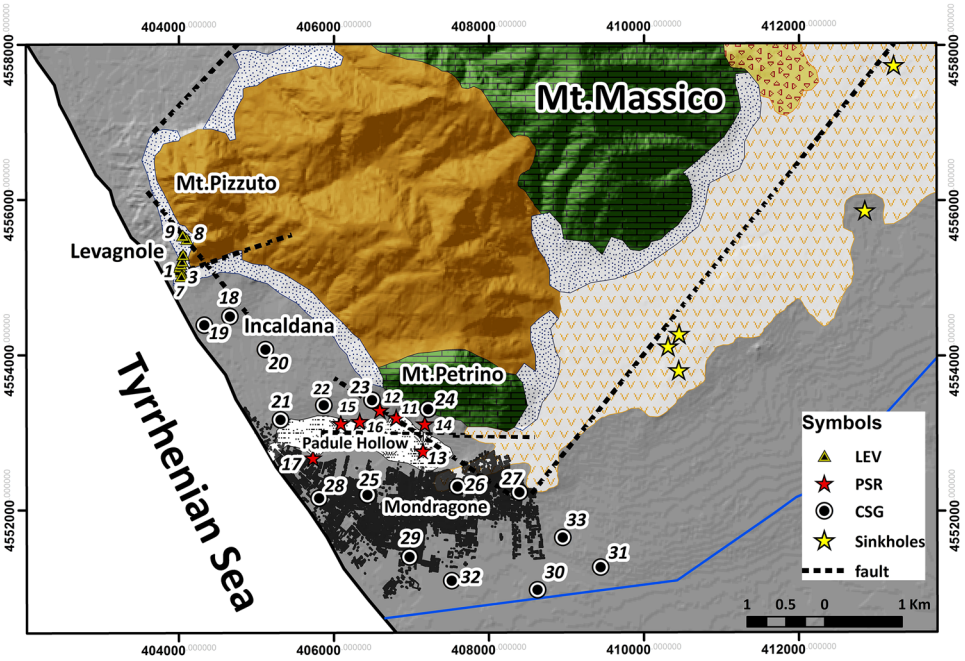

Fig. 3 Sampling site locations in the Mondragone Plain. The Levagnole (LEV) system is located at the foot of Mt. Pizzuto, whereas the Padule-S. Rocco (PSR) system is located in the Padule Hollow at the foot of Mt. Petrino

and D/H ratios were acquired from Corniello et al. (2015). All data for waters are reported in Table 1.

Free gas samples were collected with an upside-down funnel connected to pre-evacuated 100 mL borosilicate flasks by mean of silicone/Tygon® tubes; samplers were equipped with a Teflon stopcock and filled with 40 mL of NaOH 4 N. The water vapour fraction was not assumed as a significant component of the sample due to the relatively low temperature; therefore, the chemical composition of gases is reported in Table 2 as water free. The chemical composition of free gases and δ^{13}C-CO_2 were analysed at the Department of Earth Sciences (University of Florence) by methods described in Tassi et al. (2006, 2009). The concentrations of N_2, O_2, H_2, He, Ne, CH_4, and Ar were measured from the headspace of flasks using a Shimadzu 15 A gas chromatograph equipped with a 10 m-long 5 A molecular sieve column and a thermal conductivity detector. Concentrations of CO_2 were determined in the soda fraction by automatic titration with a 0.1 N HCl solution. The $^{13}C/^{12}C$ ratio of C in CO_2 (hereafter expressed as δ^{13}C-CO_2 ‰ VPDB) was determined by mass spectrometry, after a two-step extraction and purification procedure of the gas mixtures using liquid N_2 and a mixture of liquid N_2 and trichloroethylene. During the period of analysis, internal (San Vincenzo marble, recommended value: 1.58% VPDB) and international (NBS 19 carbonate, recommended value: 1.95% VPDB) standards produced values of 1.59 ± 0.04 and 1.95 ± 0.06, respectively.

The ^{3}He/^{4}He isotopic ratio was determined at the Environmental and Earth Sciences Department (Rochester University, USA) by the method reported in Tedesco et al. (2010). Samples were analysed on a VG 5400 Rare Gas Mass Spectrometer fitted with a Faraday cup and a Johnston electron multiplier for sequential analyses of ^{4}He (Faraday cup) and ^{3}He (multiplier) beams. Analytical error for He isotope determination was <0.3%. The ^{3}He/^{4}He ratio (R) was corrected for the addition of air using the standard He/Ne ratio (Craig and Lupton 1976). Analytical data for chemical and isotopic compositions of gas samples are reported in Table 2.

Results

Statistical behaviour of chemical variables in the water samples

Significant differences (p value <0.01) in temperature and EC_{20} have been observed among the three described sampled groups: LEV: 27–47 °C and 3953–5840 µS/cm; PSR: 21–32 °C and 1488–5360 µS/cm; CSG: 14–21 °C and 890–1433 µS/cm, respectively. The pH of thermal waters shows significant lower values in comparison with cold waters (LEV: 6.2–6.5, PSR: 6.0–6.5 vs. CSG: 6.8–7.7, respectively). Therefore, with respect to the samples in the unconfined shallow aquifer of the Mondragone plain, the LEV and PSR thermal features are constrained by: (1) similar acidic behaviour with pH (≈6) and (2) relatively high temperature and salinity. Like, in others, volcanic areas of central-southern Italy, the acidity of thermal waters is caused by CO_2 (and H_2S) entering the deep circuits from hydrothermal systems (Nicholson 1993; Minissale 2004).

To discriminate the main geochemical processes governing the water mineralization, the Pearson's correlation coefficients (R) have been computed among all measured variables for the whole data set after the proper data transformation (Reimann et al. 2008). The Pearson's coefficient has been chosen with the aim to point out the direct ($R > 0$) and inverse ($R < 0$) relations among the variables. The correlation matrix has been reported in the annex, where the significant correlations values ($p < 0.01$) have been highlighted in bold. These are the results:

1. Temperature is in direct relationship with EC ($R = 0.85$) and in inverse relationship with pH ($R = -0.70$).
2. The concentration of conservative elements (Cl, Br, Na, B, and Li) matches the previous trend (see correlation matrices in the annex), since they attain the highest values in the thermal waters and decrease linearly in the shallow groundwater.
3. Eh and NO_3 concentrations are in direct relationship with pH ($0.60 < R < 0.76$) and inverse relationship with temperature ($-0.61 < R < -0.78$) and EC ($-0.76 < R < -0.72$). This behaviour suggests that shallow groundwater is recharged by rainwater, bringing in solution NO_3 from the soil and O_2 from the atmosphere. On the other hand, thermal waters are low in O_2 due to a deep and long lasting circulation, as confirmed by low Eh (−100 mV) if compared to CSG ($170 < Eh < 280$ mV).
4. No correlation has been found with Fe and Ba due to their not conservative behaviour in solution, being strongly dependent on Eh (Fe), adsorption, and $CaSO_4$ precipitation (Ba) (Aiuppa et al. 2000; Pokrovsky et al. 2006; Prigiobbe and Bryant 2014).

Water–rock interaction and water mixing processes

The classification of water samples is given in the Langelier–Ludwig diagram (Fig. 4). The linear trend of samples from groundwater (Ca–HCO_3 corner) towards seawater graphically explains the correlation among the main chemical parameters (see the previous section). The temperature increase is confirmed by a gradual enrichment of the Cl–SO_4 and Na–K components, starting from the usual HCO_3–Ca(Mg) composition of cold samples in

Table 1 Measured chemical parameters, $\delta^{18}O$ and δD values of collected water samples

ID	Corniello et al. (2015)	*T* (°C)	pH	EC (µS/cm)	Eh (mV)	$\delta^{18}O$	δD	HCO_3^- (mg/l)	F (mg/l)	Cl (mg/l)	Br (mg/l)	NO_3 (mg/l)	SO_4 (mg/l)	Na (mg/l)	K (mg/l)	Mg (mg/l)	Ca (mg/l)	Li (ug/l)	B (µg/l)	Ba (µg/l)	Fe (µg/l)	Mn (µg/l)	Sr (µg/l)	Rb (µg/l)
LEV1	14a (S)	47.2	6.45	5650	−108	−6.1	−38.8	1440	2.8	941	2.4	0.1	554	630	66	88	552	220	13030	64	14	11	4031	346
LEV2	14b (S)	30.0	6.38	5730	−108	−6.0	−40.4	1395	2.5	967	2.8	0.1	619	659	69	90	511	240	13020	66	85	17	4288	325
LEV3	16	45.2	6.41	5840	−136	−6.1	−39.8	1648	2.6	973	3.2	9.7	512	652	67	91	615	152	12610	57	7	24	4494	223
LEV4		32.7	6.2	3954	na	na	na	1257	2.5	945	2.8	0.7	769	572	65	87	546	134	11360	55	6	541	3375	169
LEV5		30.1	6.49	4565	na	na	na	1501	3.2	1051	2.8	0.2	657	645	69	101	559	90	6749	45	5	nd	4226	230
LEV6		26.7	6.54	4139	na	na	na	1440	2.1	818	1.8	nd	563	519	55	87	468	89	6745	28	nd	nd	3434	158
LEV7		32.4	6.4	4249	na	na	na	1659	2.7	1055	3.5	0.1	538	635	66	101	536	92	6923	44	nd	nd	4691	215
LEV8		20.8	6.64	449	313	na	na	244.1	0.2	17	0.1	2.2	21	20	4	4	70	2	23	166	1	4	193	3
LEV9		24.0	6.58	1265	303	na	na	530.9	0.5	165	0.5	2.3	86	119	13	17	148	14	224	65	nd	nd	807	4
PSR11	13	32.0	6.50	5360	−49	−6.1	−41.2	2560	2.9	727	1.8	0.2	113	479	43	164	480	80	5370	328	10	50	2030	69
PSR12	5	22.4	5.96	2175	−105	−6.1	−38.0	1136	1.3	184	0.6	0.2	73	140	20	71	235	40	1703	97	98	139	616	29
PSR13	7	23.1	6.38	2081	142	−6.4	−38.9	1098	1.9	164	0.5	0.3	21	149	29	67	204	40	641	520	2630	155	603	48
PSR14	19	25.0	6.47	1740	−29	−6.4	−38.3	911	1.8	126	0.3	7.1	41	112	23	60	196	30	513	346	164	60	499	39
PSR15	20 (S)	23.9	6.27	2754	216	−6.2	−38.8	1785	0.8	106	0.3	0.1	49	143	23	90	387	50	1099	18	4013	504	896	54
PSR16	21	20.6	6.08	1488	209	−6.7	−42.2	814	0.9	87	nd	15.8	44	92	34	34	184	20	344	23	5289	1923	524	55
PSR17	28	22.0	6.50	3010	240	−6.2	−38.5	1537	0.4	343	0.8	4.4	83	249	35	98	339	41	1568	35	795	672	1217	49
CSG18	16	18.2	6.88	1040	251	−5.4	−32.6	256	0.5	58	0.2	125	119	61	4	21	115	4	51	23	8	2	521	5
CSG19	1	16.6	7.36	953	177	−5.8	−36.3	405	0.3	47	0.3	28	40	47	7	12	132	1	86	78	16	8	464	3
CSG20	2	16.2	7.44	890	240	−5.7	−35.5	366	0.8	49	0.1	55	60	40	6	10	136	4	53	36	7	1	349	13
CSG21	3	15.8	7.36	1154	241	−5.8	−35.1	415	0.7	83	0.2	92	84	50	11	25	148	6	79	27	51	2	507	17
CSG22	4	17.6	7.42	1154	265	−5.8	−36.0	416	0.8	58	0.1	78	51	52	11	32	116	nd	167	22	20	1	427	21
CSG23		14.0	7.67	1055	260	na	na	325	1.5	51	0.1	71	164	47	27	23	138	1	104	38	13	2	285	33
CSG24	6	19.6	7.19	1080	289	−6.1	−35.8	498	1.1	61	0.2	34	48	43	12	37	110	10	125	26	4	nd	330	43
CSG25	22	19.4	6.84	1404	240	−6.1	−36.7	573	1.4	116	0.4	32	88	95	19	34	140	17	299	1	3	40	348	76
CSG26	10	18.6	7.20	912	228	−6.0	−37.1	354	1.2	46	0.1	60	54	41	13	16	107	8	141	2	14	1	384	41
CSG27	8	21.4	7.07	1210	270	−6.2	−37.9	543	1.3	67	0.2	38	73	49	10	45	148	11	126	9	2	1	444	34
CSG28	9	20.9	7.32	1082	170	−5.8	−35.1	439	0.7	87	0.2	31	51	64	10	21	125	na	na	na	na	na	na	na
CSG29	25	20.4	6.96	1433	210	−6.4	−42.4	738	1.0	89	0.2	3	55	58	15	59	157	8	208	21	85	70	642	58
CSG30	26	18.6	6.93	960	289	−5.6	−35.6	256	0.6	70	0.2	89	98	46	5	22	112	2	83	21	5	3	366	12
CSG31	27	18.4	7.09	1150	na	−6.1	−35.8	542	1.1	60	0.2	27	68	45	8	45	140	10	150	29	3	4	455	24
CSG32	11	19.4	6.94	1260	235	−6.3	−37.2	551	1.2	75	0.2	43	74	55	13	48	142	9	145	13	2	2	420	31
CSG33	12	20.2	7.20	1017	243	−5.8	−35.5	464	1.2	48	0.1	33	69	36	9	29	129	5	91	19	2	1	341	22

IDs used by Corniello et al. (2015) for the same sampling points have also been reported

Table 2 Available chemical and isotopic compositions of free gases samples collected at Mondragone and in the surroundings of the Roccamonfina volcano

ID	CO_2 %vol	Ar %vol	O_2 %vol	N_2 %vol	CH_4 %vol	H_2 %vol	He %vol	Ne %vol	^{3}He %vol	He *R*/Ra	$d^{13}C(CO_2)$ ‰ VPDB
LEV	98.72	4.50E−03	1.20E−03	1.20E+00	5.12E−02	6.70E−03	4.61E−04	6.25E−06	2.43E−10	0.39	−0.29
Suio1	98.36	5.40E−03	2.10E−03	1.48E+00	1.30E−01	1.03E−02	1.08E−03	7.41E−06	7.52E−10	0.51	0.90
Suio2	98.13	4.50E−03	5.60E−03	1.66E+00	1.59E−01	1.09E−02	1.15E−03	8.85E−06	7.38E−10	0.47	1.04
Riardo	99.60	5.60E−03	6.00E−03	3.24E−01	7.40E−03	1.55E−03	3.39E−03	2.07E−03	8.72E−09	1.89	−0.65
PSR11	95.65	4.60E−02	3.00E−02	3.77E+00	8.00E−03	1.00E−04	2.28E−02	1.53E−03	5.96E−08	1.92	−1.45
PSR12	–	–	–	–	–	–	–	–	–	1.87	−1.65
PSR13	–	–	–	–	–	–	–	–	–	1.99	−2.21
PSR15	–	–	–	–	–	–	–	–	–	1.98	−1.68
Falciano	–	–	–	–	–	–	–	–	–	1.35	–
Francolise	–	–	–	–	–	–	–	–	–	1.90	–
Furnolo	–	–	–	–	–	–	–	–	–	1.88	–
Teano Caldarelle	–	–	–	–	–	–	–	–	–	1.95	–

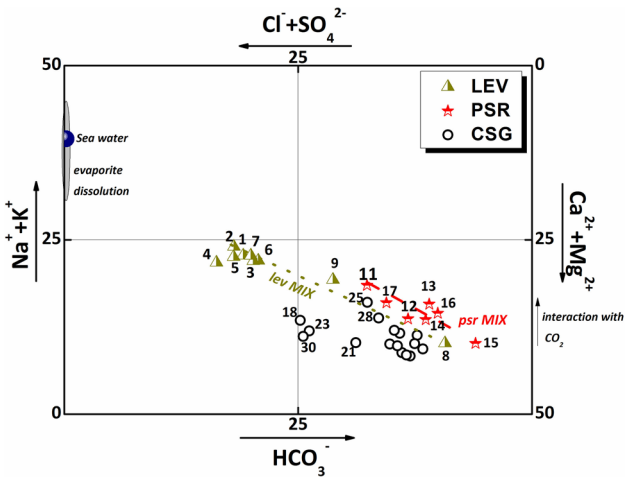

Fig. 4 Ludwig–Langelier diagram of the analysed water samples. Two different mixing trends with shallow HCO_3-rich aquifers can be observed for the thermal spring systems

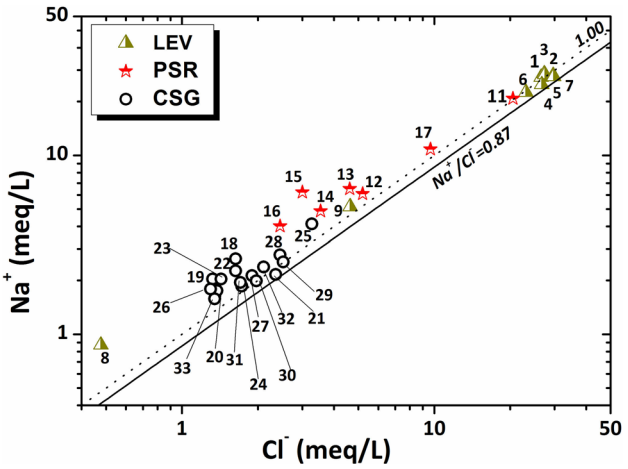

Fig. 5 Na vs. Cl diagram. Reference Na/Cl ratios are 0.87 for seawater, and 1.00 for halite dissolution. With increasing salinity, the ratio tends to 1

Italy. The waters with the highest temperatures spring out by normal faults (see Figs. 2, 3) that act as vertical conduit for the thermal fluids. The mixing trend can be independently observed for both the LEV samples (LEV mix) and the PSR samples (PSR mix).

In the LEV mix trend of Fig. 4, the non-thermal end-member is the Ca–HCO_3 shallow groundwater #9 of Mt. Pizzuto. The thermal end-member of LEV is significantly different from that of PSR waters. PSR thermal end-member is #11, taken from the deepest borehole in the area. The mixing between the PSR thermal end-member and the local shallow groundwater results in Ca–HCO_3 waters, with a percentage of alkali ions of 20–30%. CSG samples in Fig. 4 have a composition similar to PSR samples, but with lower alkali percentage.

To evaluate both the role of the lithologies involved in the leaching process and the mixing process between different aquifers, the Na vs. Cl molar concentrations are shown in a log–log diagram in Fig. 5. The diagram shows the characteristic lines of seawater ratio (Na/Cl = 0.87) and halite dissolution (Na/Cl = 1.00). Groundwater samples from carbonate aquifers (LEV and PSR) align along the Na/Cl ratio ~1, while shallow waters interacting with the volcanic rocks have a Na/Cl ratios >1 (in agreement with Larsen et al. 2001).

CSG samples from the *Incaldana* area (CSG #18, #19, #20, #22, and #23) do not seem to be influenced by the inflow of thermal waters; in fact, these samples plot with

an independent Na/Cl ratio (1.3 < Na/Cl < 1.6), which can be due to the interaction of groundwater with quaternary coastal sediments and, to a minor extent, with the underlying volcanic formations, particularly rich in alkaline elements (Duchi et al. 1995). Similarly, CSG #24 placed upstream of the PSR spring system, and CSG 27, 30, 31, 32, and 33 placed south of the investigated area, do not suggest mixing with thermal waters.

Isotopic composition of water samples

δD vs. $\delta^{18}O$ values of sampled waters have been plotted in Fig. 6. Thermal LEV and PSR samples show values smaller (δD from −42.2 to −38.0‰ SMOW and $\delta^{18}O$ from −6.0 to −6.5‰ SMOW) than the ones of the shallow CSG samples (δD from −32.6 to −42.4‰ SMOW and $\delta^{18}O$ from −5.4 to −6.4‰ SMOW). Most samples lie between the Global Meteoric Water Line (GMWL; Craig 1963) and the Mediterranean Meteoric Water Line (Gat and Carmi 1970), with δD and $\delta^{18}O$ compositions that can be related to elevations of rainfall infiltration lower than 500/700 m (Minissale and Vaselli 2011). The heaviest δD and $\delta^{18}O$ values are detected for the shallow CSG samples, which do not show mixing evidences with thermal waters, likely receiving the recharging water by the direct infiltration of rain in the Mondragone Plain. LEV thermal samples show a slight $\delta^{18}O$ positive shift (LEV2 and LEV3) with respect to the GMWL, similarly to the PSR11 thermal sample, suggesting a certain oxygen-18 exchange with rocks after long circulation, even at temperatures not necessarily high (<100 °C; e.g., Minissale et al. 2008).

By comparing the results showed in the Langelier–Ludwig diagram of Fig. 4 with the patterns reported in Figs. 5 and 6, it may be supposed that the chemistry of the thermal aquifer might be influenced by actual marine intrusion, in addition to halite dissolution. The calculated mixing (Albarede 2009) from a cold meteoric end-member on the GMWL line (δD = −44‰ and $\delta^{18}O$ = −6.8‰) and the Mediterranean Sea water (δD = +9.8‰ and $\delta^{18}O$ = +1.33‰; Shinohara and Matsuo 1986) suggests less than 5% of seawater input into the thermal LEV aquifer. This finding is in agreement with the results reported by Cuoco et al. (2015) and Corniello et al. (2015), where conservative ions were used for the mixing computation. To support such hypothesis, the $\delta^{18}O$-Cl diagram and the Cl-B diagram are shown in Fig. 7a, b, respectively. Seawater mixing with groundwater generates the $\delta^{18}O$-Cl trend and the relative mixing percentage reported in Fig. 7a. On the other hand, in Fig. 7b, the correlation does not follow a simple mixing trend with seawater. In fact, samples from shallow aquifers have a Cl/B ratio (ppm/ppb) between 0.5 and 1; with increasing salinity, seawater attains a Cl/B = 4.5, while for thermal sample, Cl/B decreases up to

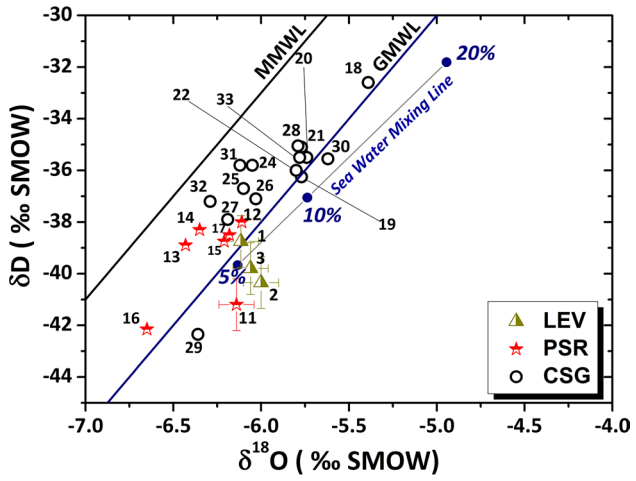

Fig. 6 $\delta^{18}O$-δD correlation diagram. The lightest isotopic values are attributed to an inland infiltration of rainfalls at altitude of 500/700 m (Minissale and Vaseli 2011)

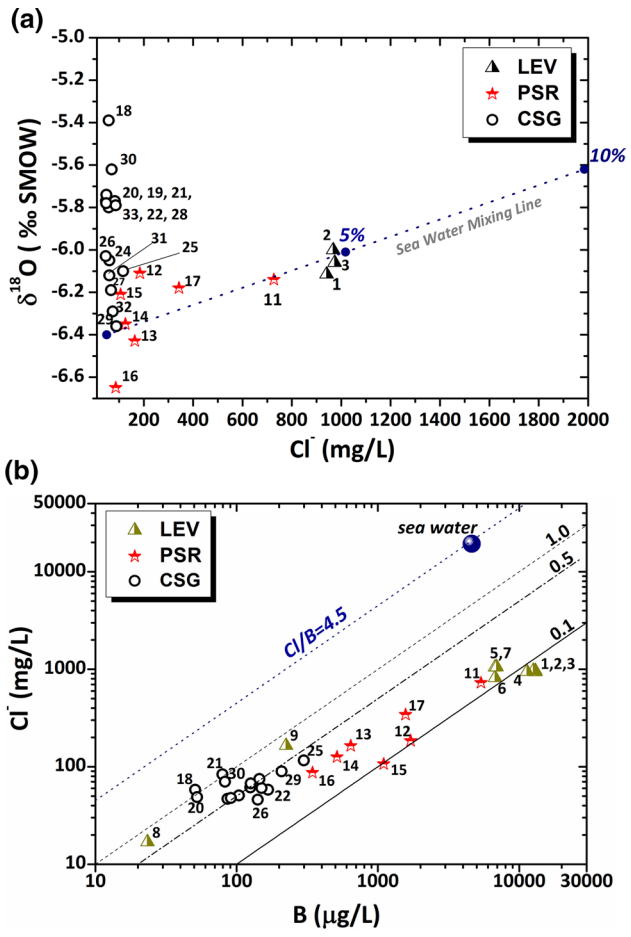

Fig. 7 Evaluation of seawater contamination of thermal reservoirs using the d18O vs. Cl diagram (**a**) and Cl vs. B diagram (**b**). The seawater mixing line is shown with relative mixing percentages (see text)

0.1. Since both Cl and B are conservative elements (Davidson and Bassett 1993), in the Peri-Tyrrhenian hydrothermal systems, they are related to the interaction with evaporite and terrigenous (clay-rich) formations, rather than to simple seawater mixing (Minissale et al. 1997, 2002; Bianchini et al. 2005). Similarly to B, also Li (240 µg/L) and Rb (120 µg/L) attain concentrations higher than seawater (Li 170 µg/L; Rb 120 µg/L), and this again suggests a contribution from water–rock interaction, as already suggested by the small oxygen-18 shift of thermal samples shown in Fig. 6. Therefore, the results of Fig. 7b suggest that in LEV and PSR thermal systems, the leaching of silicic Miocene formations generates the described enrichment. The main mineralization process of waters in thermal reservoirs seems to be caused by the interaction between water and the sedimentary host rocks, whereas the input (mixing) of 5% from seawater intrusion remains uncertain, although possible.

Chemical and isotopic composition of free gases samples

The chemical composition (in % by vol.) and the isotopic composition ($^3He/^4He$ ratio as *R*/Ra and $\delta^{13}C$-CO_2 in ‰-VPDB) of gas samples collected from the highest temperature gas bubbling waters of PSR and LEV have been reported in Table 2. To relate the results of the Mondragone area to a regional geodynamic context, data of gases collected around the Roccamonfina Volcano (location in Figs. 1, 2) have also been reported (i.e.: Suio, Riardo, Teano, Francolise and Falciano del Massico) in Table 2.

All the compositions are dominated by CO_2, either for samples located at the edge of the Garigliano Plain (Suio and LEV), or in the northern branch of the Volturno river (Fig. 2) and the Riardo Plains (PSR and Riardo, respectively). These different localities are clearly identifiable in the N_2–Ar–He ternary diagram of Fig. 8 (after Giggenbach et al. 1983), where the sample compositions are compared with some end-members, including air and air-saturated water (ASW). The PSR and Riardo gases plot near the He corner, where both mantle and crustal gases may have high He contents with an altered mantle $^3He/^4He$ signature, anyhow different from the LEV and Suio samples. LEV and Suio show a N_2 excess ($270 < N_2/Ar < 370$) with respect to air (39) or ASW (83) and to PSR and Riardo samples ($58 < N_2/Ar < 82$), which well matches with the significant increase in H_2 and CH_4 amounts of 0.007–0.01% and 0.05–0.016%, respectively (see Table 2). H_2 and CH_4 can derive from gas–gas reactions, such as the Fisher–Trops reaction ($CO_2 + 3H_2 = CH_4 + H_2O$), and re-equilibrations in rock-mineral buffered geothermal systems inside the buried carbonate reservoir (Minissale et al. 1997; Tassi et al. 2012).

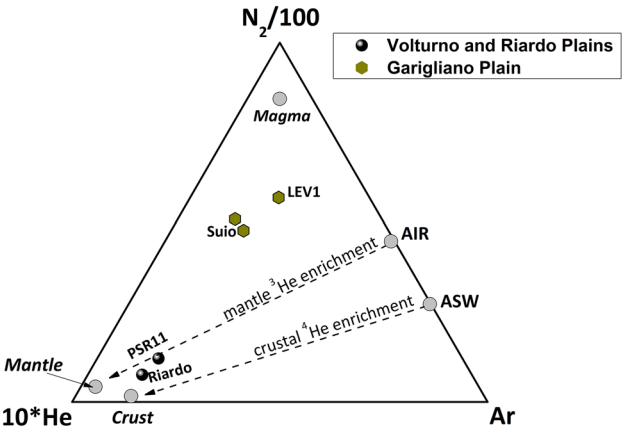

Fig. 8 Relative N_2/100-HeX10-Ar composition (Giggenbach et al. 1983) in the gas samples of the study area. Samples from Garigliano Plain (Levagnole (LEV) and Suio) show a different relative composition from the gas emissions collected at Riardo and Volturno Plains [Padule-S. Rocco (PSR) and Riardo]. These results suggest a different source of hydrothermal fluids in the two areas

In the absence of nitrogen isotopic compositions, the N_2 excess detected at Garigliano Plain might either be related to the residual activity of a magma intrusion in the carbonate basement or organic, biogenic-derived nitrogen. Differently, the low concentrations of CH_4 (0.0074–0.0080%) and H_2 (lower than 0.0016%) in the gases sampled south of Roccamonfina and Mt. Massico can be explained with a scrubbing effect of reactive gases, likely operated by deep aquifers hosted in the carbonate basement.

The relative position of samples showed in Fig. 8 can be further explained considering the isotopic compositions of He and $\delta^{13}C$ of CO_2. The relation between *R*/Ra and $CO_2/^3He$ reported in the binary diagram of Fig. 9 (O'Nions and Oxburgh 1988) allows evaluating the relations among gases deriving from different sources. In this diagram, the defined Tyrrhenian mantle *R*/Ra end-member (~6.5; Tedesco and Scarsi 1999) is enclosed in the European Sub-Continental Mantle (ESCM) value of Braüer et al. (2004). It is generally agreed that the westward subduction of the Ionian-Adriatic slab below the Apennines generates a crustal contamination in the upper mantle rising gas, giving an *R*/Ra value in the emitted gases lower than pure ESCM (Tedesco 1997). The *R*/Ra (almost 2.0) found in the Mondragone Plain, south of Mt. Massico and Roccamonfina Volcano, and in several other gases along the tectonic ORL alignment Olona Roccamonfina Line (see Fig. 1; Table 2), is only slightly lower than the He isotopic ratios measured in gases collected in the Neapolitan area at the Solfatara crater and more generally in the Pozzuoli Bay (from 2.0 to 3.0 *R*/Ra; Tedesco 1997), suggesting a common mantle wedge source. However, the samples collected at LEV, only few kilometres further north, have *R*/Ra ratios from 0.5 to

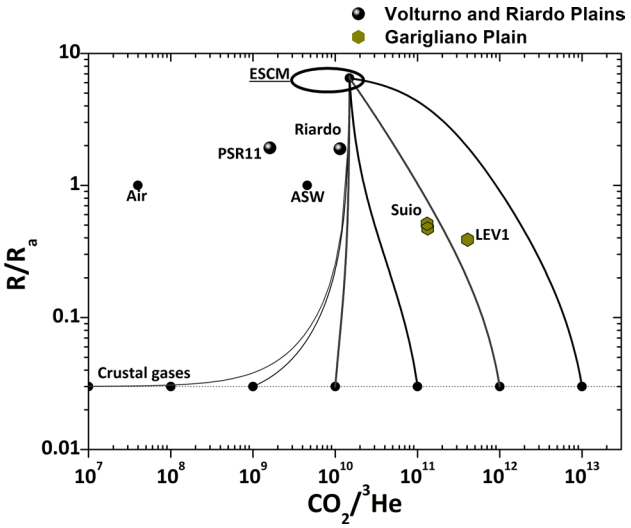

Fig. 9 $CO_2/^3He$ vs. *R*/Ra binary diagram (O'Nions and Oxburg 1998). Lines are mixing functions of a mantle component with ^4He-enriched crustal gases having $CO_2/^3He$ ratios between 10^7 and 10^{13}. Mantle end-member area is related to the specific Peri-Tyrrhenian area geodynamics (ESCM stands for European Sub-Continental Mantle). This diagram clearly shows that PSR and LEV gases belong to two different mantle wedges

1.0, a range similar to the values detected for the northern Latial volcanism (Barberi et al. 2007; Chiodini et al. 2007; Cinti et al. 2011), which definitely show the presence of two different magmatic (mantle) sources, respectively, north and south of ORL.

The $CO_2/^3He$ ratio is a useful tool to detect CO_2 addition from sources other than mantle (e.g., thermo-metamorphic) and/or CO_2 sequestration by shallow aquifers due to the high solubility of CO_2. In Fig. 9, the position of air, ASW, and mixing lines between the mantle end-member (ESMC) and crustal gases with typical *R*/Ra = 0.03 ratio have been reported, confirming the different sources (or processes) that justify the relative position if samples in Fig. 8 for the two described areas. The decreasing of $CO_2/^3He$ ratios from the mixing lines values is explained with CO_2 sequestration into the huge and confined aquifers hosted in the carbonate basement due to the higher solubility of CO_2 than He (Liotta and Martelli 2012). Gilfillan et al. (2009) and Lollar and Ballentine (2009) detected a systematic decrease in $CO_2/^3He$ with increasing Ne and He, in similar geodynamic environments. The decrease of $CO_2/^3He$ ratios at PSR and Riardo matches well the higher Ne concentration (1×10^{-3}–2×10^{-3}% by vol.) in these areas, with respect to LEV and Suio (6×10^{-6}–9×10^{-6}%, see Table 2), and thus the proposed explanation seems reliable. On the other hand, the samples from LEV1 and Suio plot along the mixing lines with $CO_2/^3He$ ratios between 10^{11} and 10^{13}, confirming their different source from PSR and Riardo. $CO_2/^3He$ in excess than mantle values are typically produced by the addition of crustal hydrothermal and/or metamorphic CO_2 (Ballentine and Burnard 2002).

The $\delta^{13}C$ of carbon in CO_2-VPDB data in Table 2 are in agreement with the previously reported hypothesis. The $\delta^{13}C$-CO_2 ranges from −1.0 to +2.0‰ VPDB (Craig 1963) for carbon deriving from limestone dissolution, while mantle-derived CO_2 ranges from −7.0 to −3.0‰ (Javoy et al. 1982; Rollinson 1993); more negative values than −δ10‰ (up to −25‰) are generally due to biogenic and bacterial-derived CO_2 (Clark and Fritz 1997). Suio and LEV samples are between −0.3 and 1.0‰, supporting the hypothesis of dissolution and/or thermo-metamorphism of carbonates, in agreement with the detected isotopic composition of natural CO_2 emissions in central-southern Italy (Panichi and Tongiorgi 1976; Minissale et al. 1997). The same context can be associated with PSR and Riardo samples, with a slight more negative $\delta^{13}C$-CO_2 range ($-0.6 < \delta^{13}C\text{-}CO_2 < -2.2$‰), which can be explained with a partial scrubbing process operated by the aquifers, as detected by Tedesco et al. (2010 and references therein) for the Lake Kivu region (Democratic Republic of Congo).

Discussion

Origin of solutes in thermal springs

The absorption of reactive gases (such as CO_2) into aquifers increases the capability of leaching of cations from the hosting rocks, leading to a water compositions that reflects the chemistry and mineralogy of the parent lithology (Giggenbach 1988; Wang and Jaffe 2004). Chemical results confirm the origin of thermal waters from circulation in deep carbonate aquifers, in agreement with the previous investigations (Corniello et al. 2015; Cuoco et al. 2015). If chemistry of PSR water samples is compared to LEV water samples, the salinity is lower, but the ratio among dissolved elements is similar, as confirmed by the relations observed in the binary diagrams in Figs. 4, 5, and 7b. This suggests that the waters are deriving from similar water-gas-rock interaction processes in similar lithologies, i.e., Mesozoic limestone and Miocene terrigenous formations.

The detected linear relationships, with a significant correlation (*R*) in the whole data set, suggest that in the study area, mixing processes involve thermal rising waters and descending meteoric-derived groundwater of the shallow aquifer(s). In the LEV system, the shallow aquifer sample (LEV8) comes from clay-rich sediments of the debris formations at the west side of Mt. Pizzuto; on the other hand, the PSR thermal water mixes with the cold groundwater hosted in the shallow formations of the Mondragone Plain (CSG).

The heavier δD and $\delta^{18}O$ values are detected for the shallow CSG samples, which do not show mixing evidences with thermal waters, likely receiving the recharging water by the direct infiltration of rain in the Mondragone Plain. Isotopic data related to the highest temperature waters are more negative, suggesting that the recharge area(s) of the deep aquifer is located at higher altitudes in inland zones, possibly in the high carbonate mountains surrounding to the east the Mondragone plain, thus suggesting that thermal waters undergo a long flow-path in the carbonate basement before emerging in the Mondragone Plain. The intermediate values between CSG and the highest temperature springs confirm the mixing processes detected through chemical data.

Gas sources and relationship with the regional hydrothermal emissions

The He isotopic compositions in the gas emissions, clearly, separate the hydrothermal systems at the Garigliano Plain (LEV and Suio), which is related to the mantle wedge belonging to the Latial province, from the southern hydrothermal manifestations at the northern edge of the Campanian and Riardo Plains, which are related to magma arising from the Campanian mantle wedge. According to what described in the previous paragraphs, the Mondragone area is the point of convergence of two distinct deep hydrothermal systems, which are springing at the southern and northern edges of Mt. Massico and Roccamonfina reliefs, respectively (Figs. 1, 2). It is widely accepted that this tectonic setting was produced by the lithosphere rifting due to the extensive tectonic activity, which triggered the formation of the Roccamonfina volcano (Capuano et al. 1992; De Rita and Giordano 1996). At the same time, the NW–SE ORL regional lineament (Fig. 1) seems to separate two different magmatic provinces, as suggested by the different chemical composition of the volcanic products belonging to the Ventotene Island (Fig. 1) and the Roman volcanic Province, which have a magmatic activity with higher crustal contamination than the volcanites produced by the Campanian eruptive centres of Vesuvious, Campi Flegrei (Solfatara), and Ischia Island (Serri 1990). On the other side, Rouchon et al. (2008) explained the evolution in time of the chemistry of the Roccamonfina volcano as a "rearrangement" of the magmatic chamber, likely produced by magma inputs supplied by different mantle sources.

As mentioned, PSR thermal springs are placed at only 3.5 km southeast of LEV springs, again in a different hydrothermal system. The consistence of the He isotopic compositions with all the CO_2-rich springs aligned on the proposed NE–SW direction (#2, #3, #4, and #5 in Fig. 2) validate the hypothesis of gases rising from a deep SW-NE linear source. Normal NE-SW fault systems likely act as the "conduits" of fluids toward the surface, as for magmas in the past, as confirmed in Fig. 2 by the good alignment with lateral spatter cones of the Roccamonfina Volcano and the basalt dike of Mt. Cesima (Di Girolamo et al. 1991). Accordingly, De Alteriis et al. (2006), Aiello et al. (2011), and Torrente and Milia (2013) suggested the presence of buried lavas in the northern Campanian Plain, which have been explained with magma arising along the normal faults in the carbonate basement. This widespread volcanic activity in the Campanian Plain could explain the occurrence of the several CO_2 rich springs far from the Roccamonfina Volcano, not only at PSR and LEV but also at Falciano del Massico and Triflisco (Fig. 1). All the gas phases associated with these mineral springs have *R*/Ra values close to 2.0, pointing out the same source for the whole Campanian Plain.

Conceptual model of fluids circulation

In agreement with the general model proposed by Minissale (2004) for the origin and circulation of the CO_2-rich thermal waters of central-southern Italy, in the Volturno and Riardo Plains, the deep rising hydrothermal fluids strongly interact with meteoric-originated waters hosted in the regional Mesozoic carbonate aquifer (Minissale et al. 2002). A conceptual scheme of this fluid circulation in the Mondragone Plain is illustrated in Fig. 10. The carbonate basement outline has been reproduced considering geophysical data presented in Billi et al. (1997). The thickness of the overlying younger formation is shown in Fig. 10b, where the schematic section reproduces the shallow geothermal dynamic of the PSR system (Amoresano et al. 2015; Corniello et al. 2015), which is similar to all the other springs in the other areas of the Campanian plain (Corniello et al. 2014).

Geophysical data from the previous investigations (Billi et al. 1997; De Alteriis et al. 2006; Aiello et al. 2011; Torrente and Milia 2013) suggest that in this area, magma intrusions in the crust are highly probable. As stated, the deep sources are different at north of the Mt. Massico horst (Latial Mantle Wedge) and at south of it (Campanian Mantle Wedge), respectively. In both sectors, the reservoirs hosted in the carbonate basement are hot and saturated by hydrothermal gases. Particularly faulted structures and in weak tectonic conditions, the flowing towards the surface of thermal water is enhanced. In fact, all the CO_2-rich springs in the area are located on at the base of the horst outcropping areas at the edges of the plains, which did not underwent massive marine sedimentation and where the accumulation of volcanic pyroclastics has not prevented the normal fault systems to allow the rising of deep mineralized CO_2-rich waters.

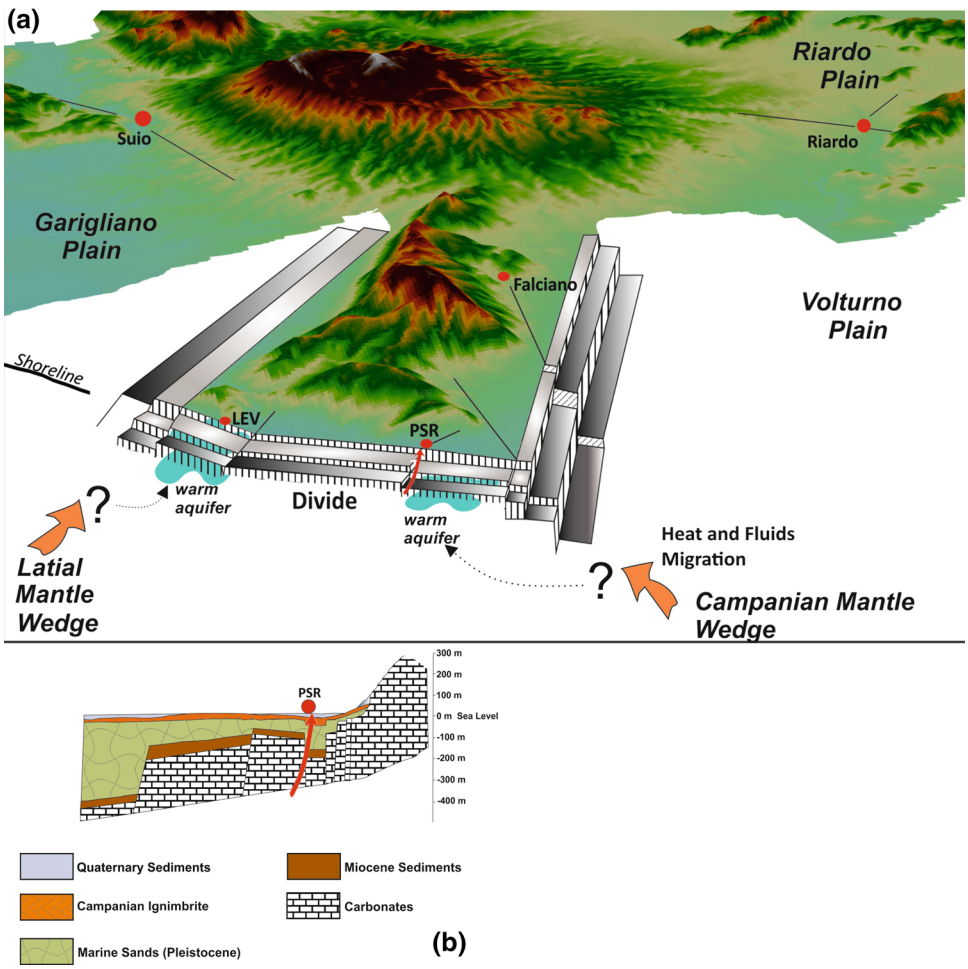

Fig. 10 Conceptual model of the fluid dynamics in the Mondragone Plain. **a** Scheme of the carbonate basement (not in scale) where warm aquifers are hosted and the fault systems, which allows the uplift of thermal waters. **b** *Vertical profile* for PSR springs (modified after Corniello et al. 2015), which is representative of the location of the carbonate basement at the foot of Mt. Petrino

The proposed model is also supported by the detected depletion of reactive gases (scrubbing) in the free gas emissions operated by the shallow aquifer hosted in the sedimentary successions. There are not available information regarding the structure and hydrodynamics of these aquifer(s), but it could be inferred that water in the deep reservoir(s) are confined, and then subject to pressurization due to both hydrostatic relation with the inland Apennine recharge zone and gas saturation. Wells drilled in the shallowest carbonate stratum in the vicinity of the natural thermal springs at PSR and Riardo produce water, as geysers with a height of almost 20 m above the ground level.

In general, the LEV and PSR systems are similar for lithologies and fluid hydrodynamics but have different heat and gas sources. The two thermal spring systems are separated by a structural divide, which do not allow the mixing among the two aquifers that emerge along fault planes, where structural conditions and ascending convective branches allow the water to rise up quickly.

Concluding remarks

Mondragone Plain thermal emergences show, at a smaller scale, the difference of the hydrothermal activities occurring at Garigliano Plain, and at Volturno and Riardo Plains. The Levagnole system and, in general, the Garigliano Plain hydrothermal fluids can be related to residual activity of a magma intrusion in the carbonates deriving from the Latial mantle wedge, which induces an higher rate of geothermal gradient than the hydrothermal manifestations at the southern sides of the Mt. Massico and Roccamonfina reliefs. In fact, in the south-eastern plains, the hydrothermal geodynamics show evidences of a deeper circulation and related volcano–tectonic events belonging to the Campanian volcanism, which also partially involves the Roccamonfina activity. Padule-S. Rocco is the westernmost inland manifestation of these geodynamics, having similar chemical evidences to the others westernmost hydrothermal sites of the Campanian and Riardo Plains (Falciano del Massico, Francolise, Teano, Riardo and Triflisco). The latter are

hosted in deep and confined aquifers. One of these aquifers is feeding, through a "fault conduit", the PSR springs at the foot of the Mt. Petrino. Even though PSR and LEV have clearly a different source, they are similar in terms of hydrogeological dynamics. Both emissions are: (1) recharged by rainwater; (2) hosted in carbonate aquifers; (3) show interaction with Miocene formations; and (4) spring out through vertical conduits, namely normal faults. The gas–water–rock interaction is the main mineralization process of water, as usual for aquifers placed at the periphery of still active hydrothermal systems. Seawater intrusion, with low mixing percentage (<5%), cannot be excluded at Levagnole, but its quantification is uncertain.

Acknowledgements The authors would thank Dr. Andrea Pietrosante for the precious instructions and helping in the GIS realization of the maps, the Prof. Micol Mastrocicco for the useful suggestions in the revision of the manuscript, and the anonymous Referees for useful suggestions to improve the quality of the manuscript.

References

Acocella V, Funiciello R (2006) Transverse systems along the extensional Tyrrhenian margin of central Italy and their influence on volcanism. Tectonics 25(2), art. no. TC2003

Aiello G, Cicchella AG, Di Fiore V, Marsella E (2011) New seismostratigraphic data of the Volturno Basin (northern Campania, Tyrrhenian margin, southern Italy): implications for tectono-stratigraphy of the Campania and Latium sedimentary basins. Ann Geophys 54(3):265–283

Aiuppa A, Allard P, D'Alessandro W, Michel A, Parello F, Treuil M, Valenza M (2000) Mobility and fluxes of major, minor and trace metals during basalt weathering and groundwater transport at Mt. Etna volcano (Sicily). Geochim Cosmochim Acta 64(11):1827–1841

Albarede F (2009) Geochemistry: an introduction. 2 Cambridge University Press, Cambridge

Amoresano A et al (2015). VIGOR: Sviluppo geotermico nella regione Campania—Studi di Fattibilità a Mondragone e Guardia Lombardi. Progetto VIGOR—Valutazione del Potenziale Geotermico delle Regioni della Convergenza, POI Energie Rinnovabili e Risparmio Energetico 2007–2013, CNR-IGG, ISBN: 9788879580151

Ballentine CJ, Burnard PG (2002) Production, release and transport of noble gases in the continental crust. Rev Min Geochem 47:481–538

Barberi F, Carapezza ML, Ranaldi M, Tarchini L (2007) Gas blowout from shallow boreholes at Fiumicino (Rome): induced hazard and evidence of deep CO_2 degassing on the Tyrrhenian margin of central Italy. J Volcanol Geothermal Res 165:17–31

Bianchini G, Pennisi M, Cioni R, Muti A, Cerbai N, Kloppmann W (2005) Hydrochemistry of the high-boron groundwaters of the Cornia aquifer (Tuscany, Italy). Geothermics 34(3):297–319

Billi A, Bosi V, De Meo A (1997) Caratterizzazione strutturale del rilievo del M. Massico nell'ambito dell'evoluzione Quaternaria delle depressioni costiere dei fiumi Garigliano e Volturno (Campania settentrionale). Il Quatenario 10(1):15–26

Bräuer K, Kämpf H, Niedermann S, Strauch G, Weise SM (2004) Evidence for a nitrogen flux directly derived from the European subcontinental mantle in the Western Eger Rift, central Europe. Geochim Cosmochim Acta 68:4935–4937

Bruno PP, Di Fiore V, Ventura G (2000) Seismic study of the '41st Parallel' fault system offshore the Campanian–Latial continental margin, Italy. Tectonophysics 324(1–2):37–55

Capuano P, Continisio R, Gasparini P (1992) Structural setting of a typical alkali-potassic volcano-Roccamonfina, southern Italy. J Volcanol Geothermal Res 53:355–369

Cataldi R, Mongelli F, Squarci P, Taffi L, Zito G, Calore C (1995) Geothermal ranking of Italian territory. Geothermics 24:115–129

Chiodini G, Baldini A, Barberi F, Carapezza ML, Cardellini C, Frondini F, Granieri D, Ranaldi M (2007) Carbon dioxide degassing at Latera caldera (Italy): evidence of geothermal reservoir and evaluation of its potential energy. J Geophys Res 112 B12204

Chiodini G, Cardellini C, Caliro S, Chiarabba C, Frondini F (2013) Advective heat transport associated with regional Earth degassing in central Apennine (Italy). Earth Planet Sci Lett 373:65–74

Cimarelli C, De, Rita D (2006) Relatively rapid emplacement of dome-forming magma inferred from strain analyses: the case of the acid Latian dome complexes (Central Italy). J Volcanol Geothermal Res 158(1–2):106–116

Cinque A, Patacca E, Scandone P, Tozzi M (1993) Quaternary kinematic evolution of Southern Appennine: relationship between surface geological features and deep lithospheric structures. Ann Geophys 36:249–260

Cinti D, Procesi M, Tassi F, Montegrossi G, Sciarra A, Vaselli O, Quattrocchi F (2011) Fluid geochemistry and geothermometry in the western sector of the Sabatini Volcanic District and the Tolfa Mts (Central Italy). Chem Geol 284:160–181

Ciotoli G, Della Seta M, Del Monte M, Fredi P, Lombardi S, Palmieri EL, Pugliese F (2003) Morphological and geochemical evidence of neotectonics in the volcanic area of Monti Vulsini (Latium, Italy). Q Intern 101–102(1):103–113

Cipollari P, Cosentino D, Gliozzi E (1999) Extension-and-compression-related basins in central Italy during the Messinian Lago-Mare event. Tectonophysics 315(1–4):163–185

Clark ID, Fritz P (1997) Environmental isotopes in hydrogeology. CRC Press, Boca Raton, FL

Conticelli S, D'Antonio M, Pinarelli L, Civetta L (2002) Source contamination and mantle heterogeneity in the genesis of Italian potassic and ultrapotassic volcanic rocks: Sr–Nd–Pb isotope data from Roman Province and Southern Tuscany. Min Petrol 74(2–4):189–222

Corniello A (1988) Considerazioni idrogeologiche su talune acque minerali e termominerali della Provincia di Caserta. Mem Soc Geol Ital 41:1053–1063

Corniello A, Ducci D, Trifuoggi M, Rotella M, Ruggieri G (2010) Hydrogeology and hydrogeochemistry of the plain between Mt. Massico and the river Volturno (Campania). Ital J Eng Geol Environ 1:51–64

Corniello A, Trifuoggi M, Ruggieri G (2014) The mineral springs of the Scrajo spa (Sorrento peninsula, Italy): a case of "natural" seawater intrusion. Environ Earth Sci 72(1):147–156

Corniello A, Cardellicchio N, Cavuoto G, Cuoco E, Ducci D, Minissale A, Mussi M, Petruccione E, Pelosi N, Rizzo E, Polemio M, Tamburrino S, Tedesco D, Tiano P, Iorio M (2015) Hydrogeological characterization of a geothermal system: the case of the thermo-mineral area of Mondragone (Campania, Italy). Intern J Environ Res 9(2):523–534

Corrado S, Aldega L, Celano AS, De Benedetti A, Giordano G (2014) Cap rock efficiency and fluid circulation of natural hydrothermal systems by means of XRD on clay minerals (Sutri, Northern Latium, Italy). Geothermics 50:180–188

Cosentino D, Federici I, Cipollari P. and Gliozzi E. (2006) Environments and tectonic instability in central Italy (Garigliano Basin)

during the late Messinian Lago–Mare episode: new data from the onshore Mondragone 1 well. Sedim Geol 188–189, 297–317

Craig H (1963) The isotopic geochemistry of water and carbon in geothermal areas. In: Tongiorgi E (ed), Nuclear geology on geothermal areas. CNR (Italian Council for Research), Spoleto, 17–54

Craig H, Lupton JE (1976) Primordial neon, helium and hydrogen in oceanic basalts. Earth Planet Sci Lett 31:369–385

Cuoco E, Verrengia G, De Francesco S, Tedesco D (2010) Hydrogeochemistry of Roccamonfina Volcano (Southern Italy). Environ Earth Sci 61:525–538

Cuoco E, De Francesco S, Tedesco D (2013a) Hydrogeochemical dynamics affecting steam-heated pools at El Chichón Crater (Chiapas—Mexico). Geofluids 13(3):331–343

Cuoco E, Spagnuolo A, Balagizi C, De Francesco S, Tassi F, Vaselli O, Tedesco D (2013b) Impact of volcanic emissions on rainwater chemistry: the case of Mt. Nyiragongo in the Virunga volcanic region (DRC). J Geochem Explor 125:69–79

Cuoco E, Tedesco D, Poreda RJ, Williams JC, De Francesco S, Balagizi C, Darrah TH (2013c) Impact of volcanic plume emissions on rain water chemistry during the January 2010 Nyamuragira eruptive event: implications for essential potable water resources. J Hazard Mater 244–245:570–581

Cuoco E, Darrah TH, Buono G, Eymold WK, Tedesco D (2015) Differentiating natural and anthropogenic impacts on water quality in a hydrothermal coastal aquifer (Mondragone Plain, Southern Italy). Environ Earth Sci 73(11):7115–7134

D'Amore F, Di Domenico A, Lombardi S (1995) Considerazioni geochimiche e geotermometriche sul sistema idrotermale di Suio (Campania). Geol Romana 31:319–328

Davidson GR, Bassett RL (1993) Application of boron isotopes for identifying contaminants such as fly ash leachate in groundwater. Environ Sci Technol 27:172–176

De Rita D, Funiciello R, Pantosti D, Salvini F, Sposato A, Della Vedova M (1986) Geological and structural characteristics of the Pontine Islands (Italy) and implications with the evolution of the Tyrrhenian margin. Mem Soc Geol Ital 36:55–65

De Rita D, Giordano G (1996) Volcanological evolution of Roccamonfina volcano (Italy): origin of the summit caldera. In: McGuire WJ et al (eds), Volcano instability on the earth and other planets. Geological Society Special Publications London 110, 209–224

De Alteriis G, Fedi M, Passaro S, Siniscalchi A (2006) Magnetoseismic interpretation of subsurface volcanism in the Gaeta Gulf (Italy, Tyrrhenian Sea). Ann Geophys 49(4–5):929–943

Del Prete S, De Riso R, Santo A (2004) Primo contributo sui sinkhole di origine naturale in Campania. Atti Conf. "Stato dell'arte sullo studio dei sinkhole e ruolo delle amministrazioni statali e locali nel governo del territorio", 20–21 May, APAT, Roma, pp 361–376

Di Filippo M, Lombardi S, Nappi G, Reimer GM, Renzulli A, Toro B (1999) Volcano-tectonic structures, gravity and helium in geothermal areas of Tuscany and Latium (Vulsini volcanic district), Italy. Geothermics 28(3):377–393

Di Girolamo P, Melluso L, Morra V (1991) Magmatic activity northeast of Roccamonfina volcano (Southern Italy): petrology, geochemistry and relationship with Campanian volcanics. Neues Jahrb Miner 163:271–289

Ducci D, Corniello A, Sellerino M (2010) Hydrostratigraphical setting and groundwater quality status in alluvial aquifers: the low Garigliano River Basin (Southern Italy), case study. In: Proceedings of conference on groundwater quality sustainability. Krakow, 12–17 Sept, pp 197–203

Duchi V, Minissale A, Vaselli O, Ancillotti M (1995) Hydrogeochemistry of the Campania region in southern Italy. J Volcanol Geothermal Res 67(4):313–328

Ferranti L, Oldow JS, Sacchi M (1995) Pre-quaternary froge-parallel extension in the Southern Appennine belt, Italy. Tectonophysics 260:325–347

Frondini F, Caliro S, Cardellini C, Chiodini G, Morgantini N, Parello F (2008) Carbon dioxide degassing from Tuscany and Northern Latium (Italy). Glob Planet Change 61(1–2):89–102

Frondini F, Caliro S, Cardellini C, Chiodini G, Morgantini N (2009) Carbon dioxide degassing and thermal energy release in the Monte Amiata volcanic-geothermal area (Italy). Appl Geochem 24(5):860–875

Gambardella B, Cardellini C, Chiodini G, Frondini F, Marini L, Ottonello G, Vetuschi Zuccolini M (2004) Fluxes of deep CO_2 in the volcanic areas of central-southern Italy. J Volcanol Geothermal Res 136(1–2):31–52

Gasparrini M, Ruggieri G, Brogi A (2013) Diagenesis versus hydrothermalism and fluid-rock interaction within the Tuscan Nappe of the Monte Amiata CO_2-rich geothermal area (Italy). Geofluids 13(2):159–179

Gat JR, Carmi I (1970) Evolution of the isotopic composition of atmospheric waters in the Mediterranean Sea area. J Geophys Res 75:3039–3048

Giggenbach WF (1988) Geothermal solute equilibria. Derivation of Na–K–Mg–Ca geoindicators. Geochim Cosmochim Acta 52(12):2749–2765

Giggenbach WF, Gonfiantini R, Jangi BL, Truesdell AH (1983) Isotopic and chemical composition of parbati valley geothermal discharges, North–West Himalaya, India. Geothermics 12(2–3):199–222

Gilfillan SMV, Lollar BS, Holland G, Blagburn D, Stevens S, Schoell M, Cassidy M, Ding Z, Zhou Z, Lacrampe-Couloume G, Ballentine CJ (2009) Solubility trapping in formation water as dominant CO_2 sink in natural gas fields. Nature 458(7238):614–618

Giordano G, Naso G, Scrocca D, Funiciello R, Catalani F (1995) Processi di estensione e circolazione di fluidi a bassa termalità nella Piana di Riardo (Caserta, Appennino Centro-Meridionale). Boll Soc Geol Ital 114:361–371

Italiano F, Martelli M, Martinelli G, Nuccio PM (2000) Geochemical evidence of melt intrusions along lithospheric faults of the Southern Apennines, Italy: geodynamic and seismogenic implications. J Geophys Res B Solid Earth 105 (B6), 13569–13578

Javoy M, Pineau F, Allegre CJ (1982) Carbon geodynamic cycle. Nature 300:171–173

Larsen D, Swihart GH, Xiao Y (2001) Hydrochemistry and isotope composition of springs in the Tecopa basin, southeastern California, USA. Chem Geol 179(1–4):17–35

Liotta M, Martelli M (2012) Dissolved gases in brackish thermal waters: an improved analytical method. Geofluids 12(3):236–244

Lollar BS, Ballentine CJ (2009) Insights into deep carbon derived from noble gases. Nat Geosci 2(8):543–547

Milano G, Di Giovambattista R, Ventura G (2008) Seismic activity in the transition zone between Southern and Central Apennines (Italy): evidences of longitudinal extension inside the Ortona–Roccamonfina tectonic line. Tectonophysics 457(1–2):102–110

Milia A, Torrente MM, Massa B, Iannace P (2013) Progressive changes in rifting directions in the Campania margin (Italy): new constrains for the Tyrrhenian Sea opening. Glob Planet Change 109:3–17

Minissale A (2004) Origin, transport and discharge of CO_2 in central Italy. Earth Sci Rev 66(1–2):89–141

Minissale A, Vaselli O (2011) Karst springs as "natural" pluviometers: constraints on the isotopic composition of rainfall in the Apennines of central Italy. Appl Geochem 26(5):838–852

Minissale A, Evans W, Magro G, Vaselli O (1997) Multiple source components in gas manifestations from north–central Italy. Chem Geol 142:175–192

Minissale A, Vaselli O, Tassi F, Magro G, Grechi GP (2002) Fluid mixing in carbonate aquifers near Rapolano (central Italy): chemical and isotopic constraints. Appl Geochem 17(10):1329–1342

Minissale A, Borrini D, Montegrossi G, Orlando A, Tassi F, Vaselli O, Delgado HA, Yang J, Cheng W, Tedesco D, Poreda R (2008) The Tianjin Geothermal Field (north-eastern China): water chemistry and possible reservoir permeability reduction phenomena. Geothermics 37:400–428

Mostardini F, Merlini S (1986) Appennino centro meridionale: sezioni geologiche e proposta di modello strutturale. Mem Soc Geol Ital 35:177–202

Nicholson K (1993) Geothermal fluids. Chemical and exploration techniques. Springer, Berlin, 236

Nicotera P, Civita M (1969) Idrogeologia della Piana del Basso Garigliano. Mem. Istituto di Geologia Applicata, Università di Napoli, vol 11-Parte II

O'Nions RK, Oxburgh ER (1988) Helium, volatile fluxes and the development of continental crust. Earth Planet Sci Lett 90(3):331–347

Ortolani F, Aprile F (1985) Principali caratteristiche stratigrafiche e strutturali dei depositi superficiali della Piana Campana. Boll Soc Geol Ital 104(2):195–206

Panichi C, Tongiorgi E (1976) Carbon Isotopic composition of CO_2 from springs, fumaroles, mofettes and travertines of Central and Southern Italy: a preliminary prospection method of Geothermal Area. In: Proceedings of second united nations symposium on the development and use of geothermal resources, San Francisco, May 1975, pp 815–825

Panza GF, Peccerillo A, Aoudia A, Farina B (2007) Geophysical and petrological modelling of the structure and composition of the crust and upper mantle in complex geodynamic settings: the Tyrrhenian Sea and surroundings. Earth Sci Rev 80(1–2):1–46

Pascale-Tommasone F, De Francesco S, Cuoco E, Verrengia G, Santoro D, Tedesco D (2011) Radon hazard in shallow groundwaters II: dry season fracture drainage and alluvial fan upwelling. Sci Total Environ 409(18):3352–3363

Peccerillo A (2001) Geochemistry and petrogenesis of quaternary magmatism in central-southern Italy. Geokhimiya 39(6):579–592

Piochi M, Bruno PP, De Astis G (2005) Relative roles of rifting tectonics and magma ascent processes: inferences from geophysical, structural, volcanological, and geochemical data for the Neapolitan volcanic region (southern Italy). Geochem Geophys Geosyst 6(7), Q07005

Pokrovsky OS, Schott J, Dupré B (2006) Trace element fractionation and transport in boreal rivers and soil porewaters of permafrost-dominated basaltic terrain in Central Siberia. Geochim Cosmochim Acta 70(13):3239–3260

Prigiobbe V, Bryant SL (2014) pH-dependent transport of metal cations in porous media. Environ Sci Technol 48(7):3752–3759

Reimann C, Filzmoser P, Garrett RG, Dutter R (2008) Statistical data analysis explained: applied environmental statistics with R. Wiley, Oxford

Rolandi G, Bellucci F, Heizler MT, Belkin HE, De Vivo B (2003) Tectonic controls on the genesis of ignimbrites from the Campanian Volcanic Zone, southern Italy. Miner Petrol 79(1–2):3–31

Rollinson H (1993) Using geochemical data. Longman Group, London

Romano P, Santo A, Voltaggio M (1994) L'evoluzione geomorfologica del Fiume Volturno (Campania) durante il tardo Quaternario (pleistocene medio-superiore-Olocene). Il Quaternario 7(1):41–59

Rouchon V, Gillot PY, Quidelleur X, Chiesa S, Floris B (2008) Temporal evolution of the Roccamonfina volcanic complex (Pleistocene), Central Italy. J Volcanol Geothermal Res 177(2):500–514

Serri G (1990) Neogene Quaternary magmatism of the Tyrrhenian region: characterization of the magma sources and geodynamic implications. Mem Soc Geol Ital 41:219–242

Shinohara H, Matsuo S (1986) Results of analyses on fumarolic gases from F-1 and F-5 fumaroles of Vulcano, Italy. Geothermics 15(2):211–215

Tassi F, Vaselli O, Moratti G, Piccardi L, Minissale A, Poreda R, Delgado Huertas A, Bendkik A, Chenakeb M, Tedesco D (2006) Fluid geochemistry versus tectonic setting: the case study of Morocco. Geol Soc Lond Spec Publ 262:131–145

Tassi F, Vaselli O, Tedesco D, Montegrossi G, Darrah T, Cuoco E, Mapendano MY, Poreda R, Delgado Huertas A (2009) Water and gas chemistry at Lake Kivu (DRC): geochemical evidence of vertical and horizontal heterogeneities in a multibasin structure. Geochem Geophys Geosyst 10, 1–22

Tassi F, Fiebig J, Vaselli O, Nocentini M (2012) Origins of methane discharging from volcanic-hydrothermal, geothermal and cold emissions in Italy. Chem Geol 310–311:36–48

Tedesco D (1997) Systematic variations in the $^3He/^4He$ ratio and carbon of fumarolic fluids from active volcanic areas in Italy: evidence for radiogenic 4He and crustal carbon addition by the subducting African plate? Earth Planet Sci Lett 151(3–4):255–269

Tedesco D, Scarsi P (1999) Intensive gas sampling of noble gases and carbon at Vulcano island (southern Italy). J Geophys Res 104:10499–10510

Tedesco D, Tassi F, Vaselli O, Poreda RJ, Darrah T, Cuoco E Yalire MM (2010) Gas isotopic signatures (He, C, and Ar) in the Lake Kivu region (western branch of the East African rift system): geodynamic and volcanological implications. J Geophys Res Solid Earth 115(1), art. no. B01205

Torrente M, Milia A (2013) Volcanism and faulting of the Campania margin (EasternTyrrhenian Sea, Italy): a three-dimensional visualization of a new volcanic field of Campi Flegrei. Bull Volcanol 75:719

Torrente MM, Milia A, Bellucci F, Rolandi G (2010) Extensional tectonics in the Campania Volcanic Zone (eastern Tyrrhenian Sea, Italy): new insights into the relationship between faulting and ignimbrite eruptions. Ital J Geosci 129(2):297–315

Wang S, Jaffe PR (2004) Dissolution of a mineral phase in potable aquifers due to CO_2 releases from deep formations; effect of dissolution kinetics. Energy Convers Manag 45(18–19):2833–2848

Zitellini N, Marani M, Borsetti A (1984) Post-orogenic tectonic evolution of Palmarola and Ventotene basins (Pontine Archipelago). Mem Soc Geol Ital 27:121–131